Controllable generation of a spin-triplet supercurrent in a Josephson spin-valve

Adrian Iovan, Taras Golod, and Vladimir M. Krasnov[1, *]

[1] *Department of Physics, Stockholm University, AlbaNova University Center, SE-10691 Stockholm, Sweden*

It has been predicted theoretically that an unconventional odd-frequency spin-triplet component of superconducting order parameter can be induced in multilayered ferromagnetic structures with non-collinear magnetization. In this work we study experimentally nano-scale devices, in which a ferromagnetic spin valve is embedded into a Josephson junction. We demonstrate two ways of in-situ analysis of such Josephson spin valves: via magnetoresistance measurements and via in-situ magnetometry based on flux quantization in the junction. We observe that supercurrent through the device depends on the relative orientation of magnetization of the two ferromagnetic layers and is enhanced in the non-collinear state of the spin valve. This provides a direct prove of controllable generation of the spin-triplet superconducting component in a ferromagnet.

arXiv:1405.4754v1 [cond-mat.supr-con] 19 May 2014

An interplay of superconductivity (S) and ferromagnetism (F) in hybrid S/F heterostructures leads to a variety of unusual physical phenomena [1–10]. Of particular interest is a possibility of generation of an unconventional odd-frequency spin-triplet component of the superconducting condensate [2, 7]. The ferromagnetic exchange energy is usually much larger than the superconducting energy gap. Consequently, a conventional spin-singlet superconducting order parameter decays at a short range ~ 1 nm in a spatially uniform, mono-domain ferromagnet. Experimental observations of a long-range proximity effect through strong ferromagnets [11, 12] and, in particular, through almost fully spin-polarized half-metals [13–15] is consistent with appearance of the spin-triplet component, which is insensitive to strong magnetic and exchange fields. However, it may also be due to various types of artifacts and, at certain circumstances, a long-range spin-singlet component can be realized in clean S/F heterostructures [9]. Therefore, unambiguous confirmation for existence of the spin-triplet superconductivity in S/F heterostructures requires controllable tunability of the phenomenon. This is also prerequisite for potential applications of S/F heterostructures in spintronics.

The spin-triplet order parameter in S/F heterostructures is generated in presence of an active spin-mixing interface [5, 7] or in case of a spatially non-uniform distribution of magnetization [2]. The latter can be achieved in spin valve structures with several F-layers [1, 3, 6, 8–10]. Both the spin-singlet and the spin-triplet components depend on the angle between magnetization of F-layers in such superconducting spin valves. The spin-singlet component is at maximum for the antiparallel (AP) and minimum at the parallel (P) state of the spin valve [9]. The spin-triplet component is maximum at the non-collinear state with 90° misalignment between magnetic moments and zero both in P- and AP-states [3, 8]. Such a behavior has been confirmed by analysis of the inverse proximity effect (i.e., suppression of superconductivity in an S-layer in contact with a ferromagnet) for F/S/F [16, 17] and S/F/F [18] structures.

Direct probing of the spin-triplet supercurrent in F-layers requires measurements of perpendicular transport properties through S/F heterostructures [6, 8–10]. Even though supercurrent in such heterostructures has been observed [19–21], a conclusive evidence for the spin-triplet nature of the supercurrent is still missing due to a difficulty with separation of singlet and triplet components and due to a general complexity of such a device with several degrees of freedom, influence of stray fields and Josephson vortices. Interpretation of the data becomes particularly difficult in case of multi-domain switching of the spin valve [4, 20]. Consequently, for unambiguous interpretation of the data it is necessary to study small mono-domain structures and to establish accurate in-situ characterization techniques.

Here we study nano-scale Josephson spin-valve devices, in which a spin valve is implemented as a barrier in a Josephson junction. We describe two methods for in-situ characterization of devices using: (i) perpendicular magnetoresistance and (ii) in-situ magnetometry based on flux quantization in a Josephson junction. This way we unambiguously prove that the critical current is enhanced in the non-collinear state of the spin valve, successfully demonstrating a controllable generation of the spin-triplet order parameter.

We study two types of Josephson spin-valves, consisting of two dissimilar CuNi ferromagnetic layers $F_{1,2}$ separated by a spacer layer of either a normal metal (N) Cu or a thin superconductor (S') Nb. Scanning electron microscope (SEM) image and a sketch of the structures are shown in Figures 1 (a) and (b). The two ferromagnetic layers are made dissimilar in order to achieve different coercive fields, required for controllable switching of magnetization in the spin valve. This is also necessary for generation of spin-triplet component of the supercurrent. In the symmetric SFFS Josephson spin valve the spin-triplet component cancels out, but in dissimilar SF_1F_2S junction it does remain finite [8].

The SF_1NF_2S (Nb/$Cu_{0.5}Ni_{0.5}$/Cu/$Cu_{0.4}Ni_{0.6}$/Nb 200/10/20/10/200 nm) and $SF_1S'F_2S$ (Nb/$Cu_{0.5}Ni_{0.5}$/Nb/$Cu_{0.4}Ni_{0.6}$/Nb 200/10/10/10/200 nm) multilayers were deposited by DC-magnetron sputtering in a single deposition cycle without breaking vacuum. The $Cu_{1-x}Ni_x$ films were deposited by

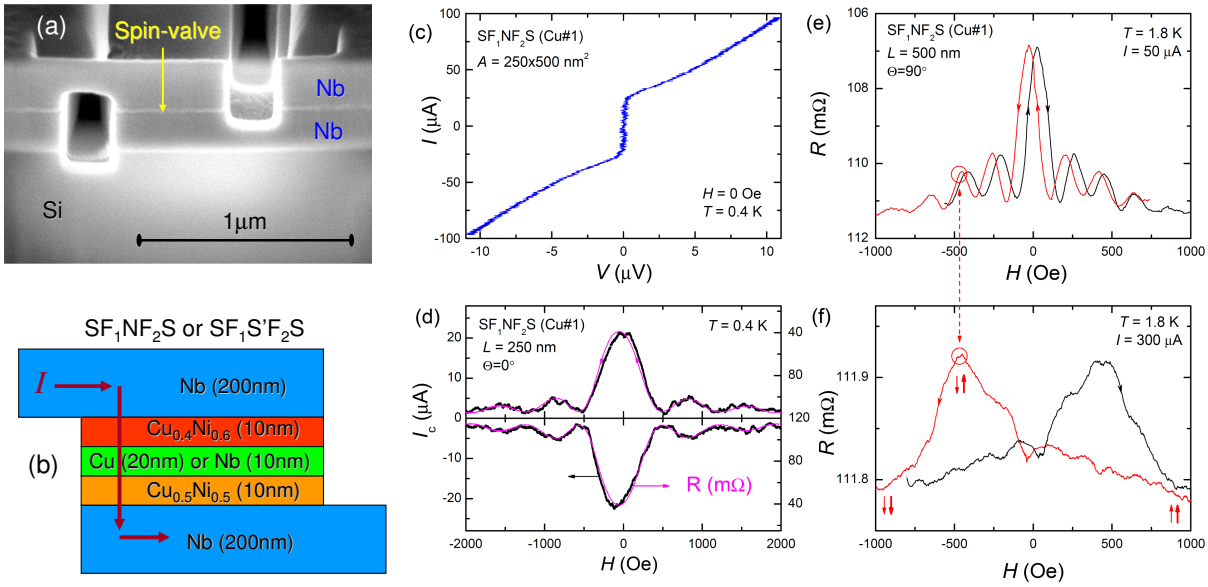

FIG. 1. **Characterization of Josephson spin valves. a,** SEM image of a device. **b,** A sketch of studied structures. **c,** Current-Voltage characteristics of a SF_1NF_2S junction (Cu#1) at zero field. **d,** Fraunhofer modulation of the Josephson current (black symbols) and a low-bias resistance (magenta lines) at $T = 0.4$ K. **e,** Low and **f,** high bias resistance of the same junction versus magnetic field for upwards (black) and downwards (red lines) field sweeps at $T = 1.8$ K. It is seen that we can study both the Josephson current and the spin-valve magnetoresistance by changing the bias level. A hysteretic behavior of the spin valve is clearly seen in both plots. Circles indicate the AP-state for the downward field sweep.

co-sputtering from Cu and Ni targets. Nano-scale junctions with sizes down to 100 nm were patterned by photolithography, reactive ion etching and three-dimensional nano-sculpturing using focused ion beam, as described in Ref. [22]. Small dimensions were necessary both for mono-domain switching of spin valves (domain size in CuNi is ~ 100 nm [23]) and for enhancement of junction resistances to comfortably measurable values. Measurements were done either in a He-3 cryostat or in a He-4 gas flow cryostat. We define the angle $\Theta = 0$ and 90° when the magnetic field is applied along and perpendicular to the long side of the junction, respectively. In all cases the magnetic field is parallel to the junction plane. In total more than ten devices were studied. The data below is representative for all of them.

Figure 1 (c) shows current-voltage (I-V) characteristics of an SF_1NF_2S junction (Cu#1 $\sim 250 \times 500$ nm^2) at $H = 0$ and $T = 0.4$ K. A critical current $I_c \simeq 25$ μA is clearly seen. It corresponds to a critical current density $J_c \simeq 2 \times 10^4$ A/cm^2. Black symbols in Fig. 1 (d) represent magnetic field dependence of the critical current at $\Theta = 0^\circ$. The field is swept from positive to negative values. A clear Fraunhofer-type $I_c(H)$ modulation proves Josephson nature of the supercurrent through a spin valve, indicates good homogeneity of I_c and a mono-domain structure of F-layers [20]. The supercurrent rapidly decreases with increasing T and becomes difficult to measure at $T > 2K$. To improve the resolution we performed lock-in measurements of resistance with a small bias of the order of I_c. The corresponding $R(H)$ modulation is shown by magenta lines in Fig. 1 (d) (right axis). It is seen that $I_c(H)$ is equivalent to the $R(H)$ data after appropriate rescaling (reverse scale, large R corresponds to small I_c). Since the noise level is much smaller for lock-in measurements, in what follows we will use low-bias resistance for characterization of I_c.

Fig. 1 (e) shows the $R(H)$ modulation for the same SF_1NF_2S junction at $\Theta = 90^\circ$ and $T = 1.8$ K. Measurements were performed with a low ac-current amplitude $I = 50$ μA. Here we can clearly see a hysteresis between the upward (black) and downward (red) field sweeps, which is due to remanence magnetization of the spin valve. At higher fields (not shown) Abrikosov vortices may be trapped in S-electrodes. As discussed in Ref. [22], vortex-induced hysteresis is opposite to remanence magnetization and, therefore, can be clearly distinguished. All the data presented here is for the vortex-free case. The absence of vortices indicates that the magnetization from F-layers do not puncture S-layers, but is forced to lie in-plane despite possible perpendicular anisotropy of magnetization in CuNi thin films [23].

Fig. 1 (f) shows the high bias resistance, measured for the same configuration as in Fig. 1 (e) but with a large ac-current $I = 300$ μA $\gg I_c$. As seen from the I-V in Fig. 1 (c) in this case we measure predominantly the normal resistance R_n at the Ohmic part of the I-V. It is seen that $R_n(H)$ represents a spin valve magneto-resistance

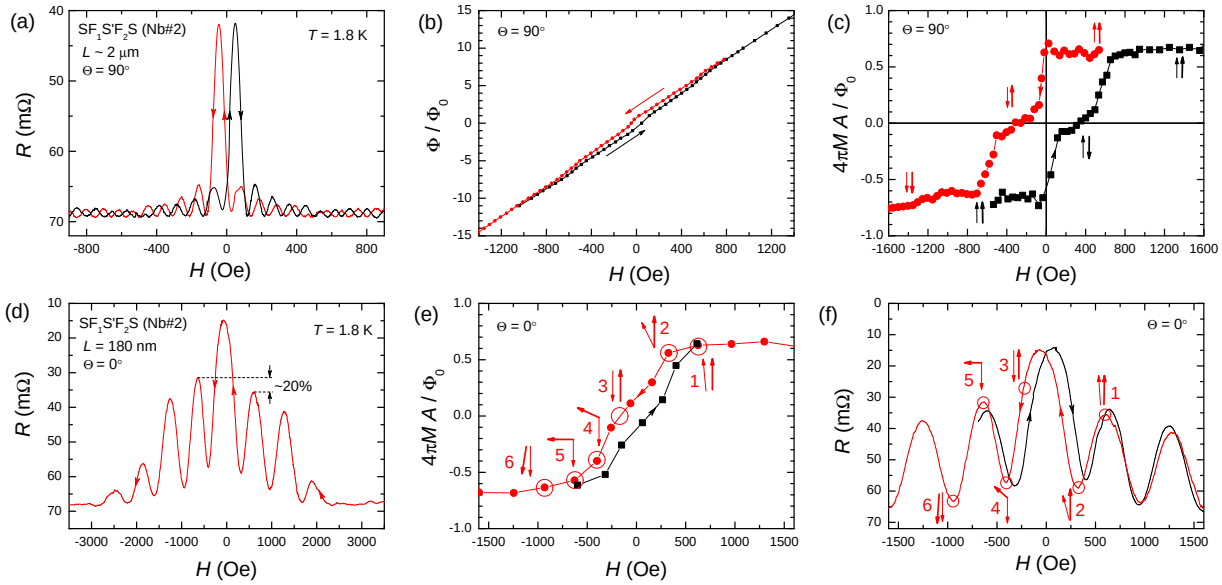

FIG. 2. **Properties of $SF_1S'F_2S$ junction: in-situ magnetometry and asymmetry of the critical current.** **a**, Fraunhofer modulation of $R(H)$ at $\Theta = 90°$ for upward (black) and downward (red line) field sweeps. **b**, Magnetic field dependencies of the flux in the junction. Each point represents integer or half-integer Φ_0, corresponding to maxima or minima in $R(H)$ from panel (a). **c**, Magnetization curves at $\Theta = 90°$, obtained from the data in panel (b). The intermediate step with $M \sim 0$ corresponds to the AP-state of the spin valve. **d**, Fraunhofer modulation of $R(H)$ at $\Theta = 0°$ for the downward field sweep. **e**, The magnetization curves at $\Theta = 0°$. Arrows indicate orientations of magnetization in the spin valve at points 1-6 for the downward field sweep. **f**, Central part of the Fraunhofer modulation of $R(H)$ at $\Theta = 0°$ for upward (black) and downward (red line) field sweeps. Note the asymmetry of the Josephson current at points 1 and 5, corresponding to the same $|\Phi/\Phi_0| = 1.5$. The asymmetry is due to generation of an additional spin-triplet component of the supercurrent in the non-collinear state of the spin valve.

with minima and maxima at P- and AP-orientations of magnetizations in the two ferromagnetic layers, respectively [19, 24]. From Figs. 1 (e) and (f) it is seen that we can measure both the critical current and the magnetoresistance by changing the bias current level. Circles in Figs. 1 (e) and (f) indicate the AP-state of the spin valve for the downward field sweep. Thus we have successfully realized the Josephson spin-valve, exhibiting both the spin valve effect and the Josephson supercurrent.

Figure 2 represents data for an $SF_1S'F_2S$ junction (Nb#2 $\sim$ 180 nm $\times 2$ μm) at $T = 1.8$ K. Figs. 2 (a) and (d) represent $I_c(H)$ (low-bias $R(H)$) modulations for magnetic field orientations perpendicular to the long $\Theta = 90°$ and the short $\Theta = 0°$ sides of the junction, respectively. Minima and maxima of $I_c(H)$ (maxima and minima of $R(H)$) correspond to integer and half-integer flux quanta Φ_0 within the junction. Due to a significant difference in dimensions we see a significant difference in flux-quantization fields for the two field orientations. Unlike SF_1NF_2S junctions (Fig. 1 (f)) the spin-valve magnetoresistance in $SF_1S'F_2S$ junctions is hardly detectable, probably due to much shorter scattering time in Nb than in Cu. Therefore, we employ a different method for determination of spin valve configuration in $SF_1S'F_2S$ junctions, following Ref. [25], in which it was demonstrated that flux quantization in a Josephson junction can be used for in-situ analysis of magnetization.

In Fig. 2 (b) we plot the flux through the junction as a function of applied magnetic field for the data from Fig. 2 (a). Here every point corresponds to a maximum or a minimum of $R(H)$. Apparently it represents the $B(H) = H + 4\pi M(H)$ curve integrated over the junction crossection area A. At high fields, when both F-layers are saturated in the P-state, the $B(H)$ becomes linear. Subtracting this linear dependence we can obtain the magnetization curve $M(H)$. Thus our junctions operate as in-situ magnetometers (absolute fluxometers) for our nano-scale spin-valves.

Figs. 2 (c) and (e) show thus obtained magnetization curves for the two field orientations. From Fig. 2 (c) it is clearly seen that upon sweeping of magnetic field the magnetization of the spin valve switches via two steps. This is a standard behavior of a spin valve with different coercive fields of the two layers [24]. First at $H \sim 200$ Oe the weakest F_1 and later at $H \sim 500$ Oe the strongest F_2 layer switches the direction of magnetization. At 200 Oe $< H <$ 500 Oe there is a plateau with $M \sim 0$. It represents the AP-state of the spin valve, as indicated in the figure. In Fig. 2 (e) the behavior is similar, even though the plateau is less defined.

Red arrows in Fig. 2 (e) indicate the configuration of magnetization of the two F layers for downward sweep-

ing of the field. At a large positive field, point-1, the spin valve is close to the up-up parallel state. At point-2 the weak layer is partly rotated and the strong layer remains in the up state. At point-3 the magnetization becomes close to zero, which implies that the weak layer has accomplished the rotation and the spin valve has switched into the AP-state. At larger negative fields points-4 and 5 the stronger layer starts to progressively rotate downwards and at point-6 the spin valve is close to the down-down parallel state. Thus we can trace the state of the spin valve from the in-situ magnetization measurement. This completes characterization of the spin valve in our junctions and we can now proceed to our main topic - discussion of controllable realization of the spin-triplet component of the supercurrent.

In Fig. 2 (f) we replot the central part of the $I_c(H)$ (inverted $R(H)$) modulation at $\Theta = 0°$, in which we marked positions and magnetization orientations for the points 1-6 from Fig. 2 (e). It is seen that for the downward field sweep (red line) the critical current at point 1, which correspond to $\Phi \simeq 1.5\Phi_0$, is smaller than at point 5, which correspond to $\Phi \simeq -1.5\Phi_0$. The asymmetry is also seen for other maxima of I_c at half-integer Φ_0 in Fig. 2 (d). For the downward field sweep all the maxima of I_c at negative fields are larger than the corresponding maxima at positive fields with the same absolute value of Φ/Φ_0. As a consequence of this asymmetry there are four lobes at the negative side and only three lobs at a positive side of the $I_c(H)$ modulation in Fig. 2 (d). The asymmetry is reversed for the upward field sweep, shown by the black line in Fig. 2 (f). For the SF_1NF_2S junction (Cu#1) the same type of asymmetry is seen from Fig. 1 (e). The field sweep direction dependent asymmetry of $I_c(H)$ was observed in all studied Josephson spin valve structures and is our central observations.

The observed left-right asymmetry of $I_c(H)$ is different from the in-built $I_c(H)$ asymmetry caused by inhomogeneity of junction parameters [26], which does not depend on the direction of the field sweep. We emphasize that such the asymmetry was not present in our SFS junctions made with the same technique and with the same dimensions, but containing only one F-layer (see e.g., Fig. 4 (b) from Ref. [22]). Consequently, the asymmetry is not the property of the individual F-layers, but is related to the history dependent orientation of the spin valve.

It is important to note that points 1 and 5 in Fig. 2 (f) correspond to exactly the same absolute value of the flux $|\Phi/\Phi_0| \simeq 1.5$. Consequently, the asymmetry is entirely due to a different orientation of magnetization in the spin valve. As shown in Figs. 2 (e) and (f) at point 1 the spin valve is close to the P-state, while at point 5 it is in the non-collinear angle state. From the theoretical analysis it follows that the spin-triplet component of supercurrent has a maximum in the non-collinear state of SF_1F_2S junction with dissimilar ferromagnets [8]. Therefore, the observed direction-dependent asymmetry of the supercurrent is consistent with a controllable generation of the spin-triplet component in our Josephson spin valves. The magnitude of asymmetry indicates that the amplitude of generated spin-triplet supercurrent is rather small, in the range of 10-20% of the main spin-singlet part of the supercurrent. This is expected because in SF_1F_2S structures the spin-triplet supercurrent is only due to dissimilarity of $F_{1,2}$ layers [8], which is not large in our case. On the other hand, the dominant singlet component is beneficial for our analysis. Singlet and triplet components of the Josephson current are harmonic and double-harmonic, correspondingly, with respect to the Josephson phase difference [8]. Therefore, the dominant spin-singlet component enables a regular, periodic in Φ_0, Fraunhofer $I_c(\Phi)$ modulation and facilitates accurate characterization of our spin-valves via in-situ fluxometry, as shown in Fig. 2 (c).

To conclude, we have successfully fabricated SF_1NF_2S and $SF_1S'F_2S$ Josephson junctions with embedded nanoscale spin valve structures. We demonstrated that such Josephson spin valves exhibit both the supercurrent and the spin-valve magnetoresistance, both of which depend on the relative orientation of magnetization of the two ferromagnetic layers. Flux quantization in such structures was employed for in-situ measurement of magnetization of the spin valve. Our main result is the observation of an asymmetry of the critical current with respect to the direction of sweeping of the magnetic field, which depends solely on the orientation of the spin valve. In the non-collinear state of the spin valve we observed an increase of the Josephson supercurrent, which we attributed to controllable generation of the spin-triplet component of the order parameter.

We are grateful to A. Rydh for assistance in experiment and Ya. Fominov for a valuable discussion. Technical support from the Core Facility in Nanotechnology at Stockholm University is gratefully acknowledged.

* E-mail: Vladimir.Krasnov@fysik.su.se

[1] A. I. Buzdin, *Rev. Mod. Phys.* **77**, 935-976 (2005).
[2] F. S. Bergeret, A. F. Volkov, and K. B. Efetov, *Rev. Mod. Phys.* **77**, 1321-1373 (2005).
[3] Ya.V. Fominov, A.A. Golubov, and M.Yu. Kupriyanov, *JETP Lett.* **77**, 510-515 (2003).
[4] Ya.M. Blanter and F.W.J. Hekking, *Phys. Rev. B* **69**, 024525 (2004).
[5] J. Kopu, M. Eschrig, J. C. Cuevas, and M. Fogelström, *Phys. Rev. B* **69**, 094501 (2004).
[6] M. Houzet and A.I. Buzdin, *Phys. Rev. B* **76**, 060504 (2007).
[7] Y. Asano, Y. Sawa, Y. Tanaka, and A.A. Golubov, *Phys. Rev. B* **76**, 224525 (2007).
[8] L. Trifunovic, Z. Popovic, and Z. Radovic, *Phys. Rev. B* **84**, 064511 (2011).

[9] A.S. Mel'nikov, A.V. Samokhvalov, S.M. Kuznetsova, and A.I. Buzdin, *Phys. Rev. Lett.* **109**, 237006 (2012).

[10] N.G. Pugach, and A.I. Buzdin, *Appl. Rev. Lett.* **101**, 242602 (2012).

[11] V.T. Petrashov, I.A. Sosnin, I. Cox, A. Parsons, and C. Troadec. *Phys. Rev. Lett.* **83**, 3281-3284 (1999).

[12] J. Wang, M. Singh, M. Tian, N. Kumar, B. Liu, C. Shi, J. K. Jain, N. Samarth, T. E. Mallouk and M.H.W. Chan, *Nature Phys.* **6**, 389-393 (2010).

[13] V. Pena, Z. Sefrioui, D. Arias, C. Leon, J. Santamaria, M. Varela, S. J. Pennycook, and J. L. Martinez. *Phys. Rev. B* **69**, 224502 (2004).

[14] R.S. Keizer, S.T.B. Goennenwein, T.M. Klapwijk, G. Miao, G. Xiao and A. Gupta, *Nature* **439**, 825-827 (2006).

[15] T. Golod, A. Rydh, V. M. Krasnov, I. Marozau, M. A. Uribe-Laverde, D. K. Satapathy, Th. Wagner, and C. Bernhard, *Phys. Rev. B* **87**, 134520 (2013).

[16] B. Li, N. Roschewsky, B.A. Assaf, M. Eich, M. Epstein-Martin, D. Heiman, M. Münzenberg, and J.S. Moodera, *Phys. Rev. Lett.* **110**, 097001 (2013).

[17] N. Banerjee, C.B. Smiet, R.G.J. Smits, A. Ozaeta, F.S. Bergeret, M.G. Blamire and J.W.A. Robinson, *Nature Commun.* **5**, 3048- (2014).

[18] P. V. Leksin, N. N. Garifyanov, I. A. Garifullin, J. Schumann, V. Kataev, O. G. Schmidt, and B. Büchner, *Phys. Rev. Lett.* **106**, 067005 (2011).

[19] C. Bell, G. Burnell, C.W. Leung, E.J. Tarte, D.-J. Kang, and M.G. Blamire, *Appl. Rev. Lett.* **84**, 1153-1155 (2004).

[20] T.S. Khaire, M.A. Khasawneh, W.P. Pratt, Jr., and N.O. Birge, *Phys. Rev. Lett.* **104**, 137002 (2010).

[21] J.W.A. Robinson, G.B. Halasz, A.I. Buzdin, and M.G. Blamire, *Phys. Rev. Lett.* **104**, 207001 (2010).

[22] T. Golod, A. Rydh, and V.M. Krasnov, *Phys. Rev. Lett.* **104**, 227003 (2010).

[23] I.S. Veshchunov, V.A. Oboznov, A.N. Rossolenko, A.S. Prokofiev, L.Ya. Vinnikov, A.Yu. Rusanov and D.V. Matveev, *JETP Lett.* **88**, 758-761 (2008).

[24] B. Dieny, V.S. Speriosu, S.S.P. Parkin, B.A. Gurney, D.R. Wilhoit, and D. Mauri, *Phys. Rev. B* **43**, 1297-1300 (1991).

[25] V.V. Bolginov, V.S. Stolyarov, D.S. Sobanin, A.L. Karpovich, and V.V. Ryazanov, *JETP Lett.* **95**, 366-371 (2012).

[26] V.M. Krasnov, V.A. Oboznov, and N.F. Pedersen, *Phys. Rev. B* **55**, 14486-14498 (1997).